SECOND SEMI-ANNUAL STATUS REPORT

NASA RESEARCH GRANT NO. NAG-1-710

for Period Covering 14 April 1987 to 13 October 1987

INTEGRATION OF DYNAMIC, AERODYNAMIC, AND STRUCTURAL OPTIMIZATION OF HELICOPTER ROTOR BLADES

by

David A. Peters
Principal Investigator

School of Aerospace Engineering
Georgia Institute of Technology
Atlanta, Georgia 30332-0150

November 2, 1987

Background

This is a report on the second six-month period of this NASA Grant. The purpose of the research is to study the integration of structural, dynamic, and aerodynamic considerations in the design-optimization process for helicopter rotor blades. This is to be done in three phases. The first phase, which represents the first year of effort and which is now completed, concentrates on improving the structural optimization of our previous work to make it more realistic and to make it more compatible with the integration of dynamic and aerodynamic effects. A second goal of the first year's effort is to make preparations for years two and three through the development of a performance and loads program.

Technical Personnel

Four technical people are working on this project. Three are being paid through the grant, and one is being supported through institute funds. The principal investigator, David A. Peters, has contributed 0.9 man-months over this six-month period (15%). A Ph.D. student, Mnaouar Chouchane, has contributed 2.0 man-months; and a post-doctoral fellow, Y.P. Cheng, has contributed 0.48 man-months. In addition, an M.S. student, Mark Fulton, has worked on the project since September 15 while being supported by a Georgia Tech Research Assistantship.

Scope of Effort

The statement of work in our original proposal lists three tasks for the first-year effort (Phase I) with the third task being the largest. Task I is to bring on-line computer codes that could perform the finite-element frequency analysis of rotor blades. This has been done, as we summarized in our first status report (April 1987). Rather than bring in an existing code that might contain "extra baggage" not needed for our effort, Dr. Cheng wrote his own code specifically geared to our purposes. Table 1 summarizes the major features of this program. Although the program is based on the theory of our previous work, this new program is advanced in several ways, as

outlined in the Table. Of particular importance is the ability to model blade discontinuities and exact hinges and links, not previously available. This program is fully documented and operational. Thus, Task I is complete.

The second task in the statement of work is to bring on-line an optimization code for the work. We have tried several (including OPT and CONMIN) and we have decided to use CONMIN. One great advantage of using this program is that it was also used in our previous work. Thus, we have a firm foundation of experience with it. Presently, we are using CONMIN routinely in all of our optimization studies. Thus, Task II is also finished.

This brings us to the heart of our research, Task III, which involves the reproduction, refinement, and extension of our previous work. The original proposal lists four goals for Task III. The first is to add explicit volume constraints on the thicknesses and lumped masses used in the optimization. This was not explicitly carried out in earlier work. The second goal is to apply the specific aeroelastic constraint that the center of mass must be forward of the quarter chord in order to prevent flutter. A third goal is to include the bending-torsion coupling due to cg-ea offset within the blade cross-section. The fourth goal is to include some very simple stress constraints. In particular, the proposal calls for the axial-stress constraint and for a simple static bending constraint. (Vibratory stress constraints are reserved for the second and third years.) We have addressed all of these goals, have completed the first three, and are in the midst of completing the fourth. In addition, as a result of trying to meet the fourth goal, we have identified an additional area of research that must be completed before we can complete the fourth goal. The discussion below details the work done including this new task.

Details of Added Optimization Task

We begin with the new research task that is crucial to this work. This task is the use of optimization to match blade section geometry (thicknesses, material properties, etc.) to the structural beam properties of each cross-section (EI's and GJ's). In our earlier work with NASA, the thickness of the

box beam at each section was chosen somewhat arbitrarily based on drawings of the blade. Then, any discrepancy between the beam properties of the box beam and those of the true blade were adjusted by the addition of lumped stiffnesses and masses to make up the difference. The blade optimization was done on the box-beam properties, and the lumped "correction" properties were assumed to be unchangeable. An exception was that torsional stiffness for which the equivalent thickness of a second cell had to be determined by trial and error. This process consumed a great deal of man power, and we decided in our new research effort that it should be automated. Thus, Dr. Cheng has developed an optimization package that chooses cross-sectional properties in such a way as to match manufacturer data on blade beam properties. This not only allows beam properties to be converted into physical properties, but it also allows the possibility of optimization based on beam properties rather than on cross-sectional dimensions. In other words, one could optimize with EI's and GJ's and then convert this optimum design to thicknesses; or one could optimize with geometrical properties as design variables.

Table 2 outlines the present manner in which this process takes place. First, we try to minimize an objective function based on the differences between desired and actual beam stiffnesses. At each step, constraints are placed on stiffness wandering (τ_i); and these constraints are tightened as we approach the desired values. In step 2, we choose the shear modulus of the skin in order to match torsional stiffness. Finally, we adjust the lumped masses and the skin density in order to optimize a cost functional based on blade inertial properties. However, as we will see in results later in this report, this procedure has a weak point. In particular, although we can easily match stiffness properties, the method occasionally puts too much material into the blade skin and not enough into the box beam. Although this poses no particular problem for the frequency constraints, it does pose a problem when we add stress constraints. When the box-beam thickness is traded off for skin thickness, then the centrifugal stresses become too large in the box beam, since the skin does not carry this load. This has hampered the application of stress constraints because it makes the initial design unfeasible.

As a result, we are now experimenting with a revised procedure, outlined in Table 3. In this procedure, the skin properties are considered uniform along the blade. The thicknesses of the box beam are then used to match the four beam thickness properties. Because there are three thicknesses and four properties, we probably will need to include the trailing-edge strip as another variable. Step 2 of Table 3 indicates that there may be a need to revise skin properties if the result is unacceptable, but this remains to be seen. Finally, we need to choose lumped masses to match inertia properties. In our new formulation, we have also recognized that rotary inertia has little impact on bending. Thus, we will only try to match the total polar moment of inertia rather than I_f and I_c separately. Again, in the inertial portion we only have two free variables that must be used to match three properties. Therefore, we may need to add one additional parameter.

Completed Optimization

Although we have had some problems with the "property optimizer" mentioned above, we have been able to complete most of the goals in Task III. This has been done on the Hughes blade since it is the most common type of articulated rotor. Table 4 shows the various stages used in this optimization process. In each stage, we include the volumetric constraint on cross-sectional properties (Fig. 2), we include the aeroelastic constraint on center of mass, and we include the torsional coupling due to cg-ae offset. The first page of this table illustrates that we begin with frequency-placement as the cost functional and bring the 3rd flap, 2nd inplane, and 4th flap into their desired windows. (Note that the 1st and 2nd flap and 1st inplane and torsion are already in their windows.) In the second phase, we bring the 5th flap and 2nd torsion into their windows. With all frequencies now within the constraints, we have a feasible solution to begin the weight optimization (third page of Table 4).

Table 5 shows the results of this three-phase optimization when the structural beam properties (EI, GJ, etc.) are used as design variables. Note that the constraint on autorotational inertia prevents any great weight savings after the optimization. This is to be expected because the goal of

the optimization is to place frequencies. The minimum-weight requirement simply prevents the optimizer from doing this by adding unnecessary mass. Table 6 shows the same optimization when the physical properties (thicknesses, etc.) are used as design variables. One can see that there is little difference between the two methodologies except that the 6th flapping frequency is moved to a different window. The second method does require fewer iterations. Figure 2 shows the final physical properties from the two methods, and Fig. 3 shows the final structural properties. One can see that the optimization based on thicknesses gives more radial variation in properties. We believe that this is due to the problems mentioned earlier with respect to property selection. One can also see the large variation in thicknesses around the r=50 station. This is also due to this selection problem. It is the very small thicknesses that give difficulties when we attempt to apply stress constraints. We believe that these problems will be eliminated with our new strategy, and we expect to be able to add the stress constraints shortly.

It should also be noted here that the inclusion of bending-torsion coupling caused other problems that we had not anticipated. In particular, because of frequency cross-overs, it was sometimes hard to track a particular mode shape and frequency to see which frequency was really in which window. This is one reason that we separated the frequency placement into three subproblems (rather than only two as in our previous work). This helped us to track modes more efficiently.

Aerodynamic Loads and Performance

In our first status report, we described the development of a performance and loads program that would include stall and that could be used in the second and third years of our study. We have continued work on this program with Mr. Chouchane taking the lead. In our efforts to push the program to higher advance ratios (and higher loads), we discovered that we could not trim the helicopter beyond an advance ratio of 0.30 to 0.35. In order to find the reason for this limitation, we re-examined the optimization that previously produced gains and time constants for the trim algorithm. Based

on this, we found that the previous solution, although adequate at low speeds, did not give optimum performance when high speeds and/or stall were present. Therefore, we have been attempting a new optimization. Figures 4a-4c show time histories of rotor controls at an advance ratio of 0.25. Five different combinations of gains (K0 and K1) and time constants (T0 and T1) were used. The objective is to reach a steady-state as soon as possible and with as little steady oscillation as possible ($\leq \pm 0.3°$). Based on this, the "+" curve seemed the best of the five. Figures 5a-5c then provide the effect of changing the gain K1 alone. Based on this, K1=.04 seemed best. Consequently, we have gone ahead with these values. However, another student, Mark Fulton, has been given the task of doing a formal optimization to find the absolute best gains for this system. He is supported by Institute funds.

Once these sub-optimum gains were determined, we were able to locate the source of our trim problems. The rotor coupling matrix in our trim algorithm was simply not accurate enough at high advance ratio. Thus, we replaced it with a more accurate set of formulas based on the work of Peters and Ormiston. Figures 6a-6c show the results at advance ratios from 0.25 to 0.39. The new coupling matrix has pushed results up to μ=0.375. Beyond that, even these advanced formulas are inadequate. Figures 7a-7b show blade response for these same cases. They show that a periodic solution with no 1/rev has indeed been obtained up to μ=0.375 but not beyond. Therefore, we are developing an adaptive control that will optimize itself during the trimming process to match the particular couplings of any flight condition. This should allow us to develop the loads data we need in future phases.

Future Work

Our primary objective now is to complete the the new cross-section optimizer so that we can apply the stress constraints. As stated in our proposal, these initial stress constraints will be based on static axial loads and on the static lift necessary to lift the aircraft (flap bending only). Our second objective is the completion of Phase II which includes the addition of performance constraints within the optimization process. In this

case, the weight objective function will be replaced by a combination of weight and performance which will result in the best payload capability for a given power. Although we will begin with hover, we cannot stop there, because most helicopters are not optimized for hover performance alone. Therefore, we will need to include forward-flight performance. Our trim and stall methodologies, developed in Phase I will be useful in this context.

Finally in Phase III, we add vibratory loads and vibratory stress constraints. Here, again, we plan to relate everything to a performance index. In particular, higher stresses imply stronger (i.e., heavier) blades; and higher vibrations also imply vibration suppression devices which are a weight penalty, as well. As for the source of these vibratory loads, we will begin with a simple load spectrum. Towards the end, however, we will apply the loads program on which we are now working.

TABLES

Table 1: Some Features of the Finite Element Program of Rotor Blade.

Elements:

1. Tapered and twisted beam elements are used.
2. Beam properties are specified at two ends of element and are varied linearly along element.
3. Lumped mass matrix with the effect of elastic offset included.
4. Stiffness terms include the following: bending, torsion, elongation, tension, kinetic energy due to inplane displacement, and "torsion-rotation" energy.

Capabilities of Program:

1. Rigid links are performed mathematically to increase efficiency of program and precision of results.
2. Discontinuity of beam properties is allowed.
3. Hinges of the blade are modeled "exactly".
4. Gradient information is calculated analytically.
5. Subspace iteration method is used to increase the efficiency of the iteration process.

Table 2: Procedures Now Used to Determine Section Properties from Given Structural Data.

* Step 1: Design variables: t, s_1, s_2, or p(skin thickness)

Objective: $w_1 (EA - EA_0)^2 + w_2 (EI_f - EI_{f0})^2 + w_3 (EI_c - EI_{c0})^2$

Constraints:

$$s_1 + s_2 < b, \qquad GJ < GJ_0$$

$$(1-\tau_2)(EA_0) < EA < (1+\tau_1)(EA_0)$$

$$(1-\tau_4)(EI_{f0}) < EI_f < (1+\tau_3)(EI_{f0})$$

$$(1-\tau_6)(EI_{c0}) < EI_c < (1+\tau_5)(EI_{c0})$$

* Step 2: Solve G(skin), so that $GJ = GJ_0$

* Step 3: Design variables: a, d, skin density.

Objective: $w_1 (m - m_0)^2 + w_2 (\rho I_f - \rho I_{f0})^2 + w_3 (\rho I_c - \rho I_{c0})^2 + w_4 (e - e_0)^2$

Constraints:

$$(1-\tau_2)(m_0) < m < (1+\tau_1)(m_0)$$

$$(1-\tau_4)(\rho I_{f0}) < \rho I_f < (1+\tau_3)(\rho I_{f0})$$

$$(1-\tau_6)(\rho I_{c0}) < \rho I_c < (1+\tau_5)(\rho I_{c0})$$

$$(1-\tau_8)(e_0) < e < (1+\tau_7)(e_0)$$

* Where w_i is weighting scalar, τ_i is tolerant value, $()_0$ is given data, $()_f$ represents quantity in flapping direction, $()_c$ represents quantity in chordwise direction, and e is elastic offset.

Table 3: Proposed Procedures to Determine Section Properties from Given Structural Data.

* Step 1: Design variables: t, s_1, s_2 (Given skin thickness & G(skin))

Objective: $w_1 (EA - EA_0)^2 + w_2 (EI_f - EI_{f0})^2 + w_3 (EI_c - EI_{c0})^2 + w_4 (GJ - GJ_0)$

Constraints:

$$s_1 + s_2 < b$$

$$(1-\tau_2)(EA_0) < EA < (1+\tau_1)(EA_0)$$

$$(1-\tau_4)(EI_{f0}) < EI_f < (1+\tau_3)(EI_{f0})$$

$$(1-\tau_6)(EI_{c0}) < EI_c < (1+\tau_5)(EI_{c0})$$

$$(1-\tau_8)(GJ_0) < GJ < (1+\tau_7)(GJ_0)$$

* Step 2: If the results from Step 1 are not acceptable, then the another skin thickness and G(skin) are selected and Step 1 is performed again. Repeated Steps 1 & 2 until reasonable data are obtained.

* Step 3: Design variables: a, d (Given skin density)

Objective: $w_1 [m - m_0]^2 + w_2 [(\rho I_f + \rho I_c) - (\rho I_{f0} + \rho I_{c0})]^2 + w_3 [e - e_0]^2$

Constraints:

$$(1-\tau_2)(m_0) < m < (1+\tau_1)(m_0)$$

$$(1-\tau_4)(\rho I_{f0}) < \rho I_f < (1+\tau_3)(\rho I_{f0})$$

$$(1-\tau_6)(\rho I_{c0}) < \rho I_c < (1+\tau_5)(\rho I_{c0})$$

$$(1-\tau_8)(e_0) < e < (1+\tau_7)(e_0)$$

Table 4: Procedures of Optimizing the Hughes Articulated Rotor Blade.

Based on:	Structural Properties	Physical Properties
Frequency placement (I)		
Design variables:	EI_f, EI_c, m, ρI_f, ρI_c	t, s_1, s_2, a, d
Constraints	$1.0 < p(\text{flapping-1st})^* < 1.5$	
	$2.3 < p(\text{flapping-2nd}) < 2.75$	
	$0.3 < p(\text{inplane-1st}) < 0.7$	
	$4.23 < p(\text{torsion-1st}) < 4.7$	
	1.2581×10^4 (mugs-in^2) < autorotation	
	side constraints on design variables	
Objective	$[p(\text{flapping-3rd}) - 4.5]^2 + [p(\text{inplane-2nd}) - 6.5]^2 + [p(\text{flapping-4th}) - 7.5]^2$	

* p = (blade natural frequency) / (rotor rotational frequency).

Table 4: Procedures of Optimizing the Hughes Articulated Rotor Blade. (Continue)

Based on:	Structural Properties	Physical Properties
Frequency placement (II)		
Design variables:	EI_f, EI_c, GJ, m, ρI_f, ρI_c	t, s_1, s_2, a, d
Constraints	$1.0 <$ p(flapping-1st) < 1.5	
	$2.3 <$ p(flapping-2nd) < 2.7	
	$4.3 <$ p(flapping-3rd) < 4.7	
	$7.3 <$ p(flapping-4th) < 7.7	
	$0.3 <$ p(inplane-1st) < 0.7	
	$6.3 <$ p(inplane-2nd) < 6.7	
	$4.25 <$ p(torsion-1st) < 4.7	$4.3 <$ p(torsion-1st) < 4.7
		$12.3 <$ p(torsion-2nd) < 12.7
	1.2581×10^4 (mugs-in^2) $<$ autorotation	
	side constraints on design variables	
Objective	([p(flapping-5th) - 11.5]^2	
	+[p(torsion-2nd) - 12.5]^2)	

Table 4: Procedures of Optimizing the Hughes Articulated Rotor Blade. (Continue)

Based on	Structural Properties	Physical Properties
Weight Minimization		
Design variables:	EI_f, EI_c, GJ, m, ρI_f, ρI_c	t, s_1, s_2, a, d
Constraints	$1.0 <$ p(flapping-1st) < 1.5	
	$2.3 <$ p(flapping-2nd) < 2.7	
	$4.3 <$ p(flapping-3rd) < 4.7	
	$7.3 <$ p(flapping-4th) < 7.7	
	$11.3 <$ p(flapping-5th) < 11.7	
	$0.3 <$ p(inplane-1st) < 0.7	
	$6.3 <$ p(inplane-2nd) < 6.7	
	$4.3 <$ p(torsion-1st) < 4.7	
	$12.3 <$ p(torsion-2nd) < 12.7	
		0. < elastic offset*
	1.2581×10^4 (mugs-in^2) < autorotation	
	side constraints on design variables	
Objective	Weight of Blade	

* Except at station 75 which originally has an elastic offset equal to -.52 and has the constraint (elastic offset > -0.54).

Table 5: Optimization Results of Hughes Blade (Structural Properties as Design Variables).

	Original	Frequency Placement(I)	Frequency Placement(II)	Weight Minimization
Weight (lbs)	203.42	217.36	217.03	193.03
Autorotation	12581.	13233.	13203.	12661.
p(inplane-1st)	0.4756	0.4820	0.4820	0.4677
p(flapping-1st)	1.0293	1.0304	1.0304	1.0257
p(flapping-2nd)	2.7451	2.6143	2.6287	2.6876
p(torsion-1st)	4.2483	4.2501	4.2563	4.3058
p(flapping-3rd)	4.9035	4.5101	4.5772	4.6979
p(inplane-2nd)	6.8914	6.5029	6.5118	6.6958
p(flapping-4th)	7.9378	7.5026	7.5923	7.5558
p(flapping-5th)	12.058	10.933	11.500	11.302
p(torsion-2nd)	12.921	12.927	12.500	12.642
p(flapping-6th)	16.996	15.521	15.921	15.484
Iterations(CONMIN)	--	21	7	49

Table 6: Optimization Results of Hughes Blade (Physical Properties as Design Variables)

	Original	Frequency Placement(I)	Frequency Placement(II)	Weight Minimization
Weight (lbs)	203.42	213.86	214.55	203.15
Autorotation	12581.	12579.	12777.	12656.
p(inplane-1st)	0.4756	0.4841	0.4824	0.4708
p(flapping-1st)	1.0293	1.0310	1.0305	1.0269
p(flapping-2nd)	2.7451	2.5801	2.6049	2.6989
p(torsion-1st)	4.2483	4.3448	4.3345	4.3014
p(flapping-3rd)	4.9035	4.5049	4.5779	4.6985
p(inplane-2nd)	6.8914	6.5020	6.5186	6.6272
p(flapping-4th)	7.9378	7.4962	7.6803	7.6934
p(flapping-5th)	12.058	11.151	11.500	11.553
p(torsion-2nd)	12.921	12.580	12.684	12.380
p(flapping-6th)	16.996	15.850	16.243	16.293
Iterations(CONMIN)	--	16	7	38

FIGURES

Figure 1: Typical Blade Section

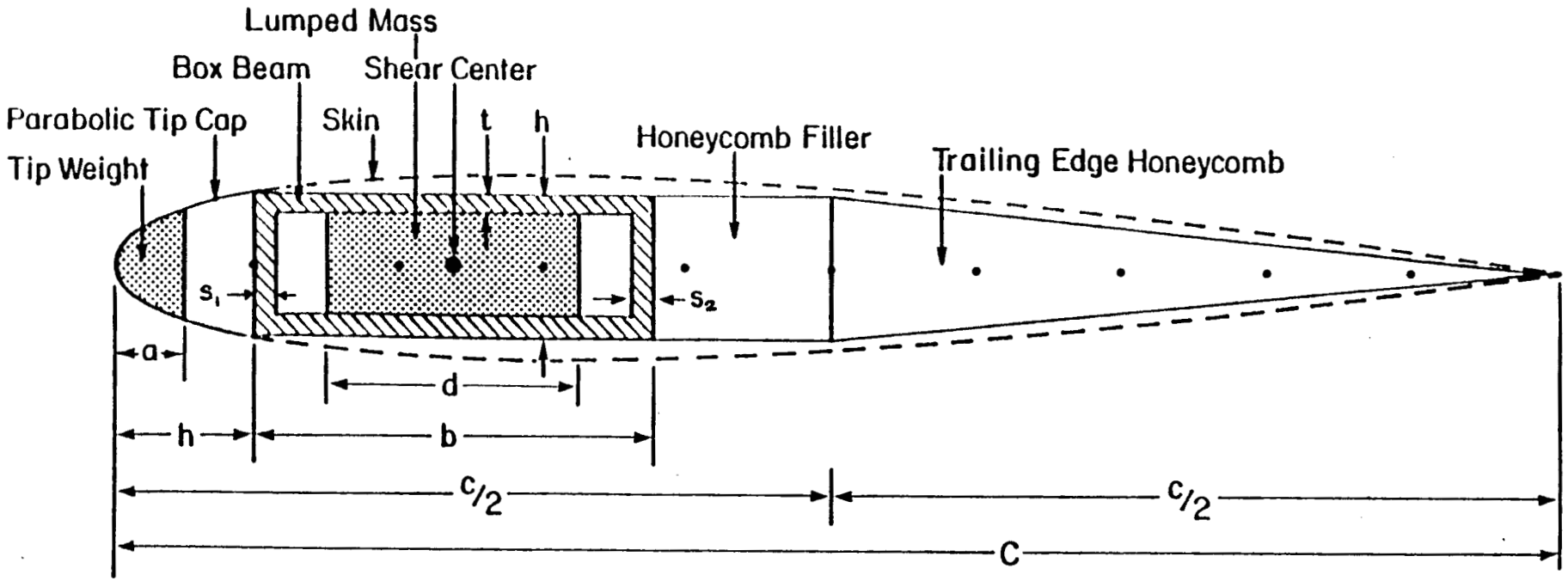

Physical properties:
t, s_1, s_2, b, a, d, c, h, p(skin thickness)

Material properties:
Density (box beam, lumped weights, & honeycomb filler)
E & G (box beam & skin)

Design variables:
t, s_1, s_2, b, a, d

Structural data:
EA, EI_f, EIc, GJ
m, ρI_f, ρI_c, e

Figure 2: Structural Data Comparison.

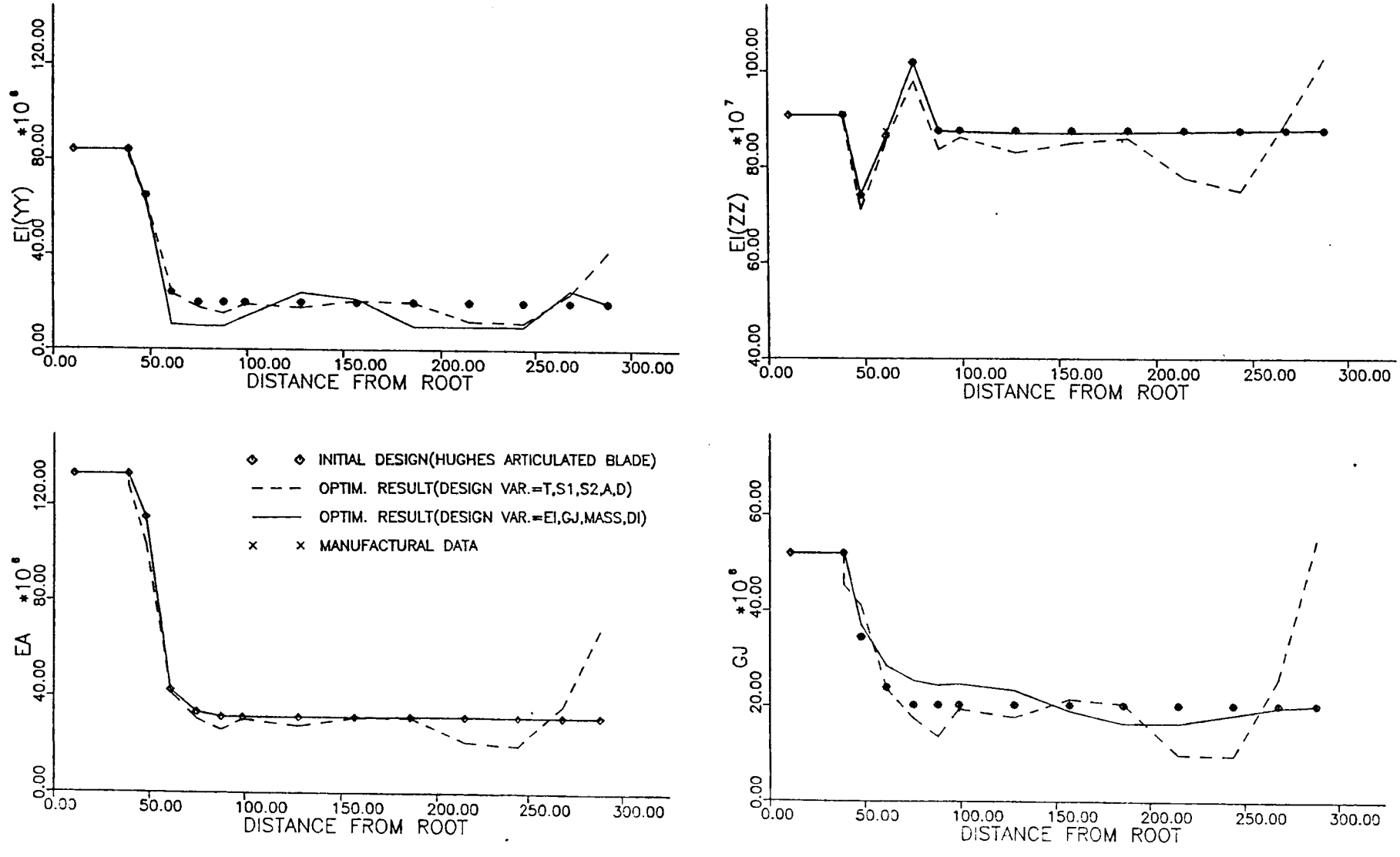

Figure 2: Structural Data Comparison (Continue)

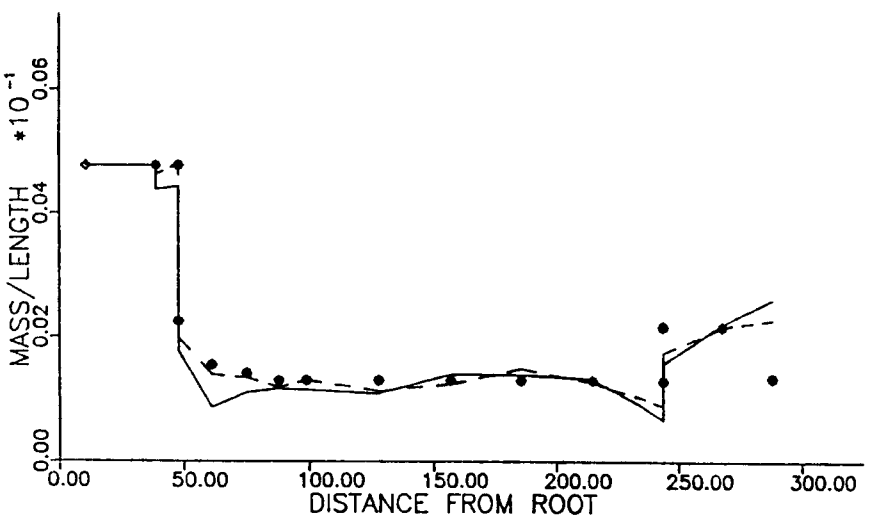

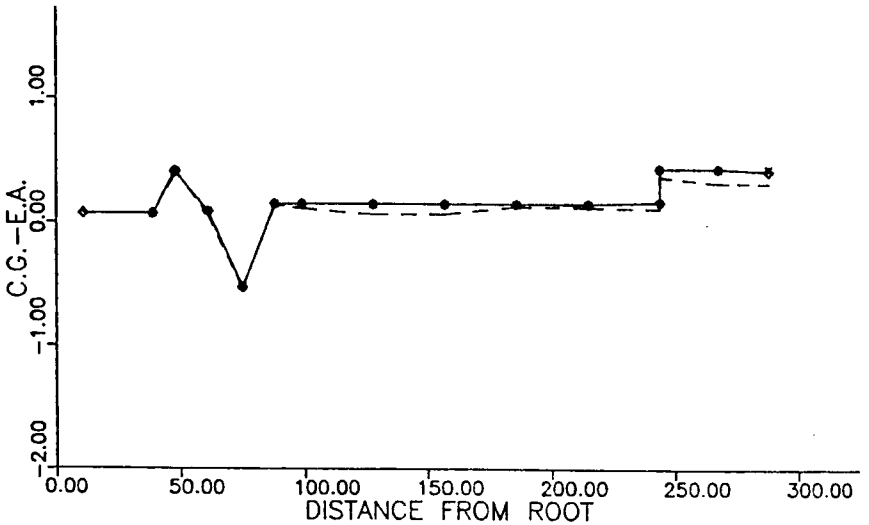

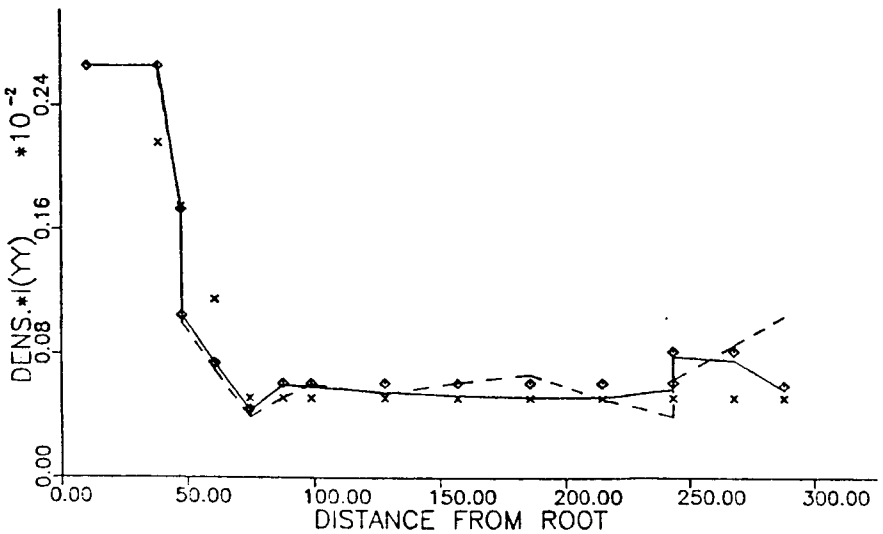

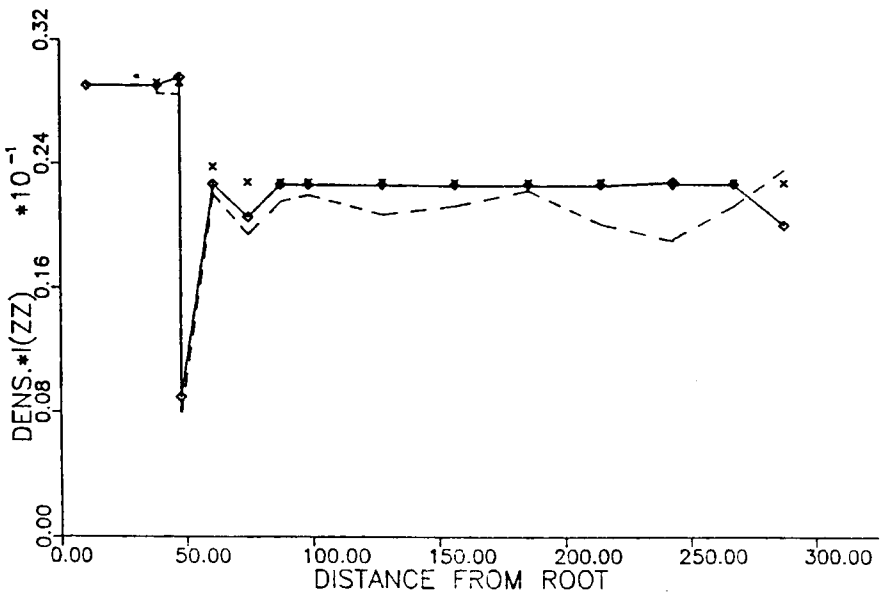

Figure 3: Section Thickness Comparison.

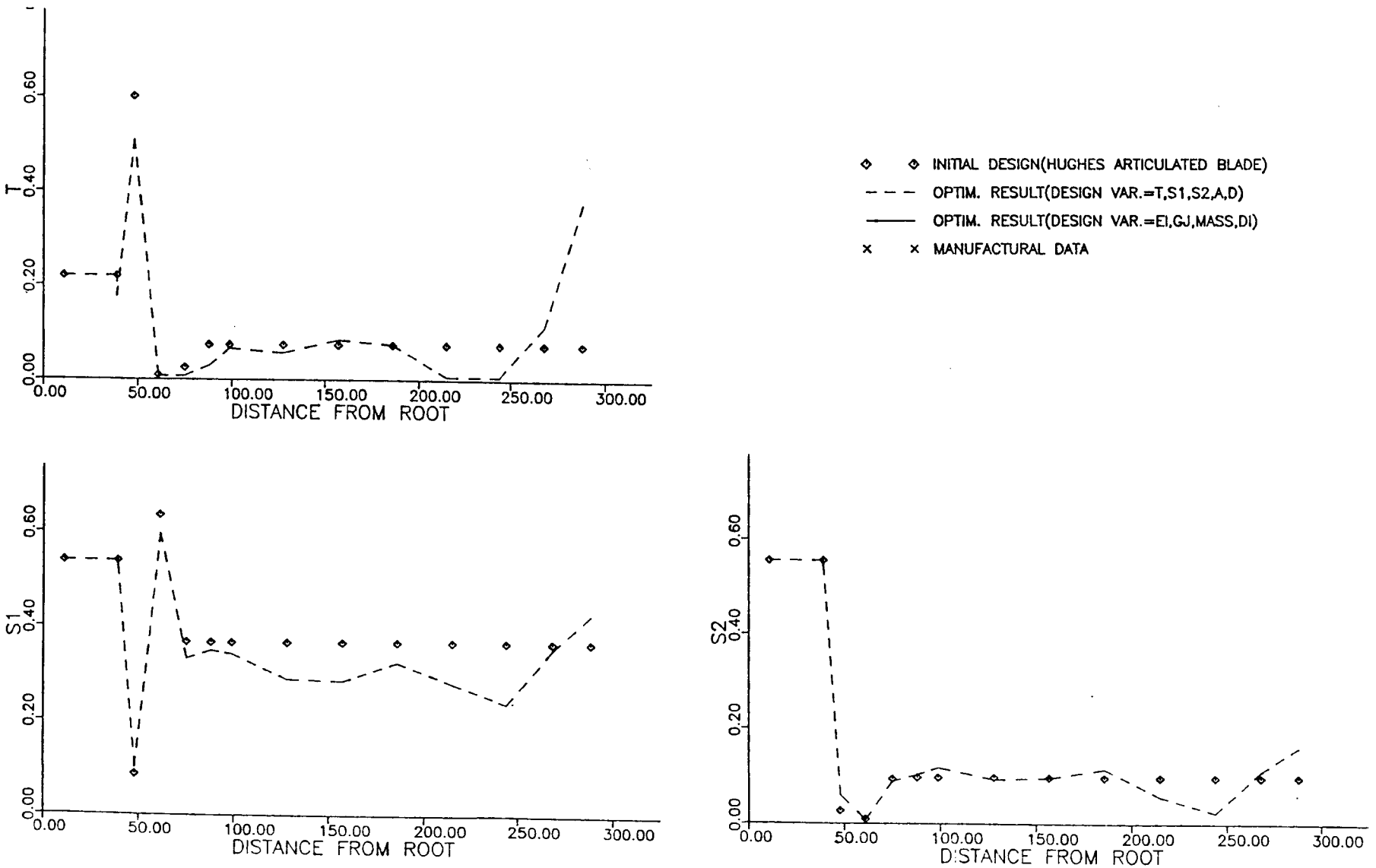

Figure 3: Section Thickness Comparison (Continue).

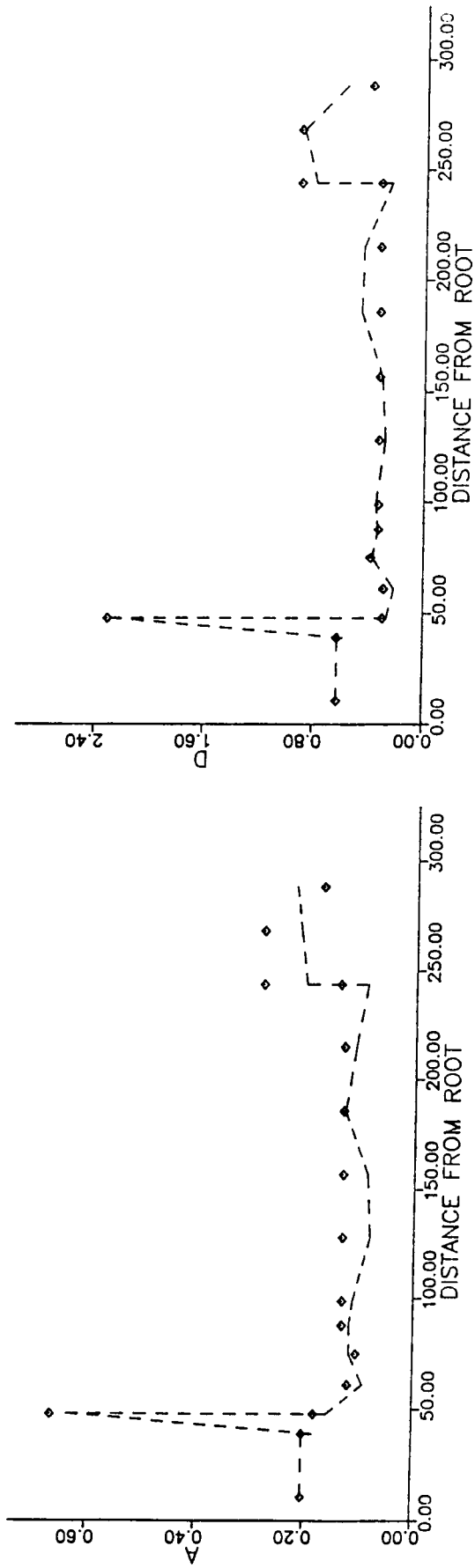

FIGURE 4a: AUTO–PILOT CONTROL MU=.25

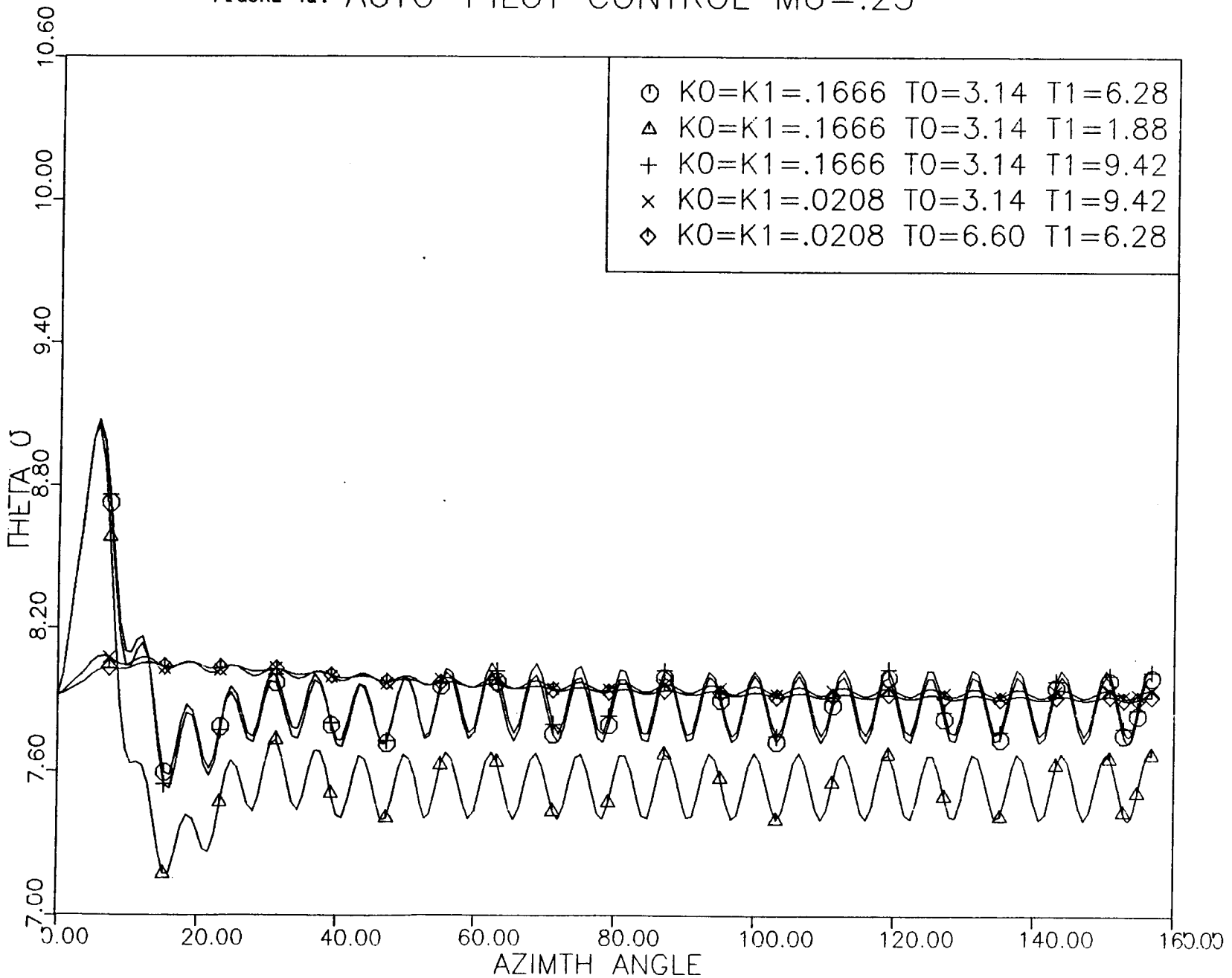

FIGURE 4b: AUTO–PILOT CONTROL MU=.25

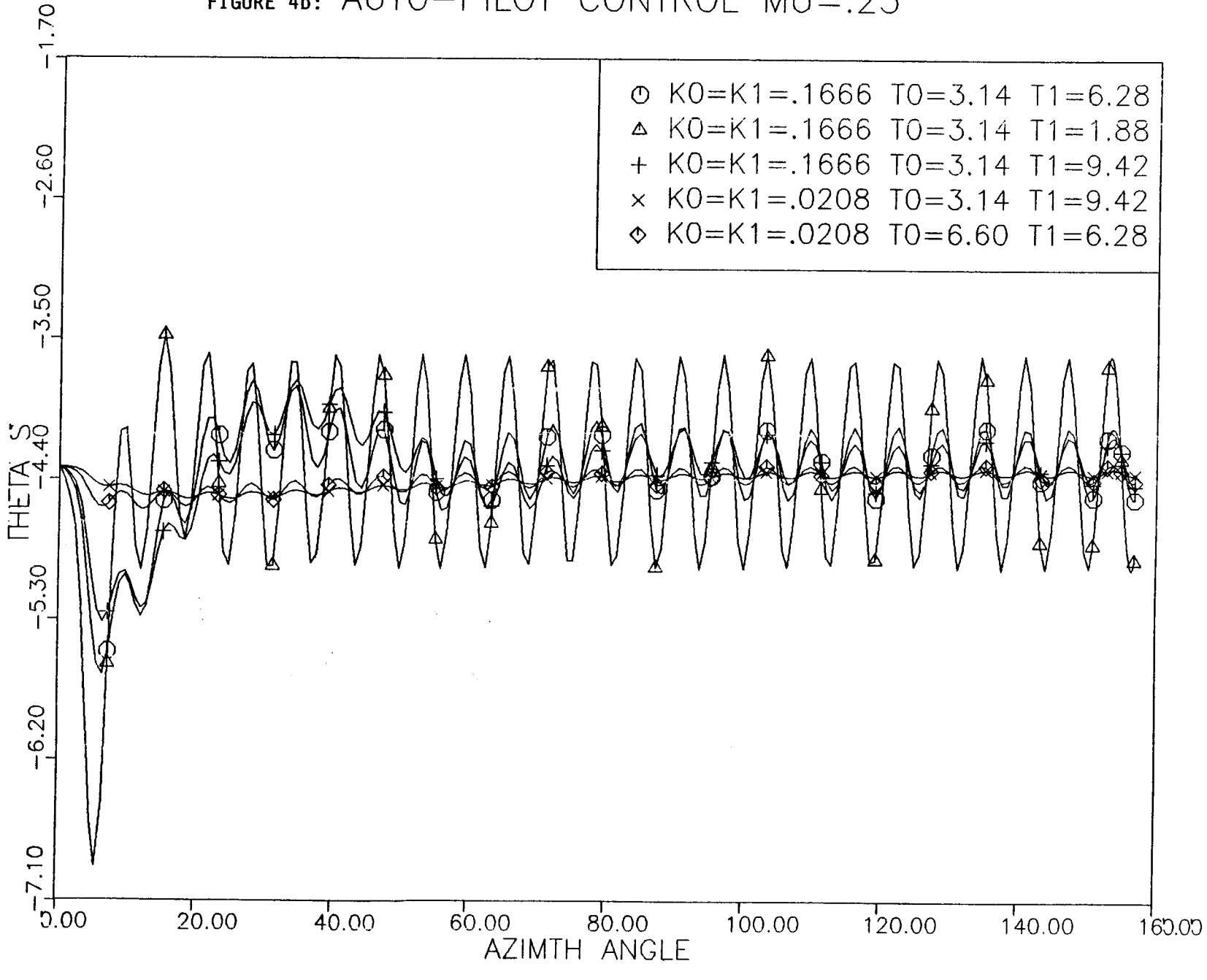

FIGURE 4c: AUTO—PILOT CONTROL MU=.25

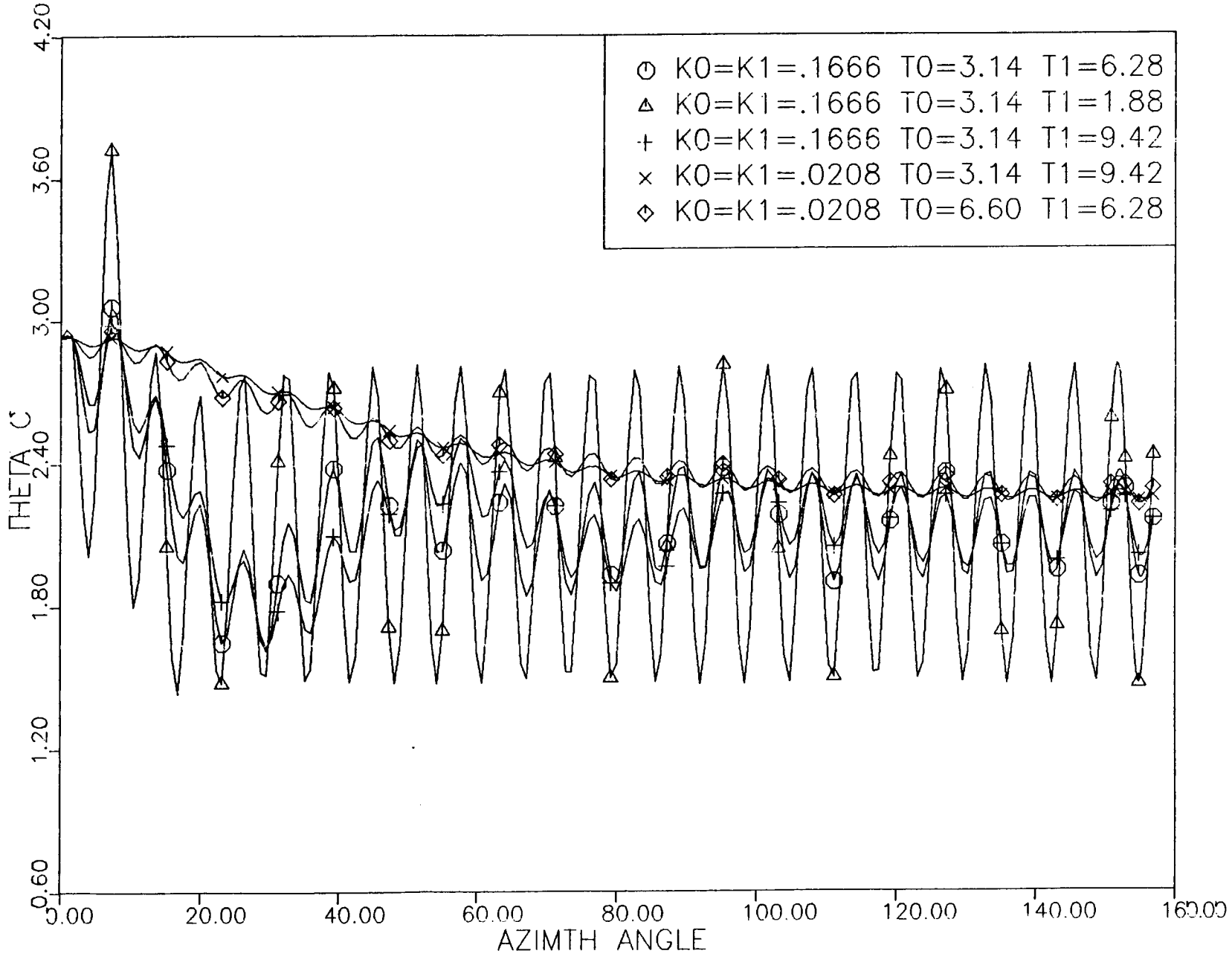

FIGURE 5a: AUTO–PILOT CONTROL

MU=.25 T0=3.1416 T1=9.425

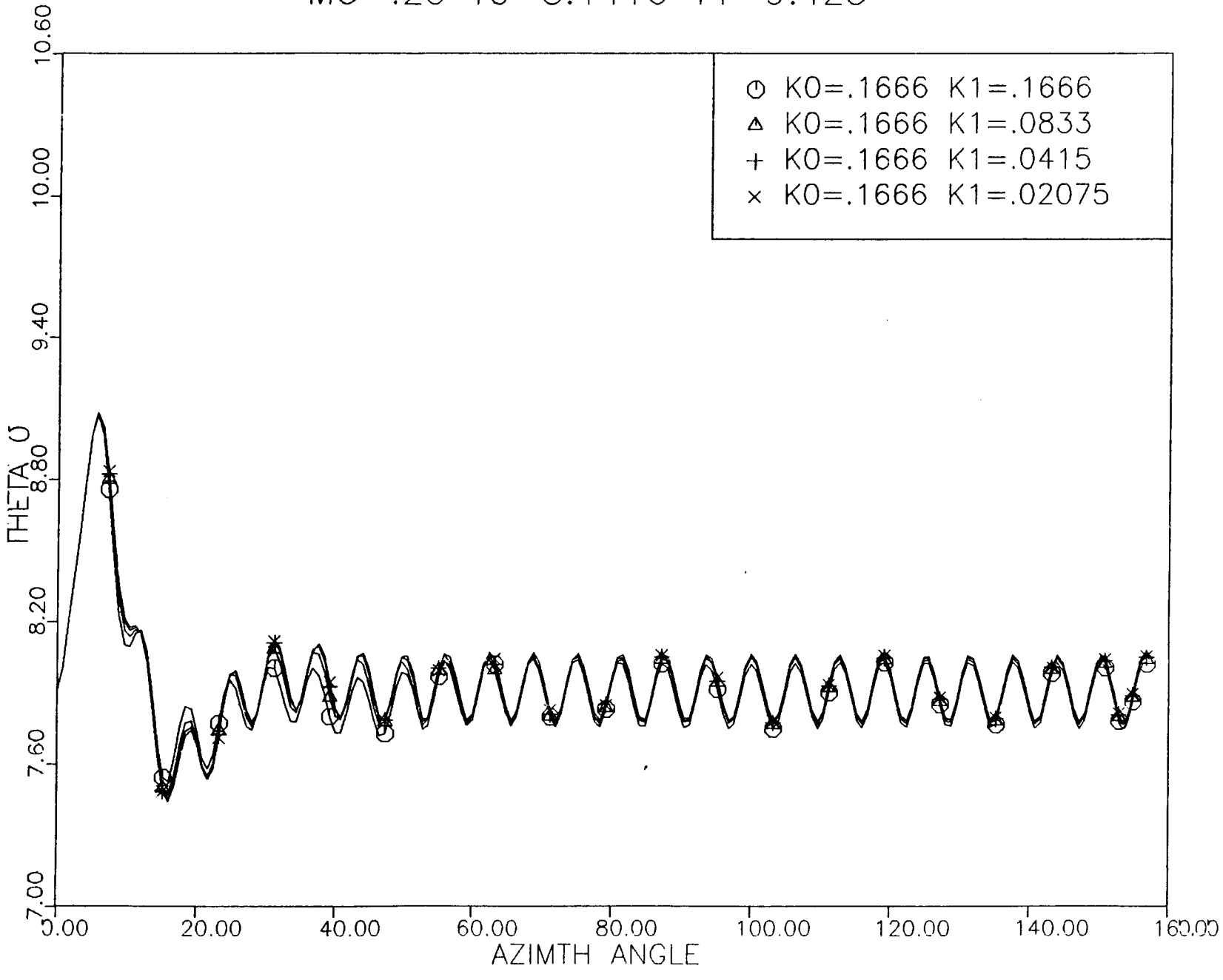

FIGURE 5b: AUTO-PILOT CONTROL
MU=.25 T0=3.1416 T1=9.425

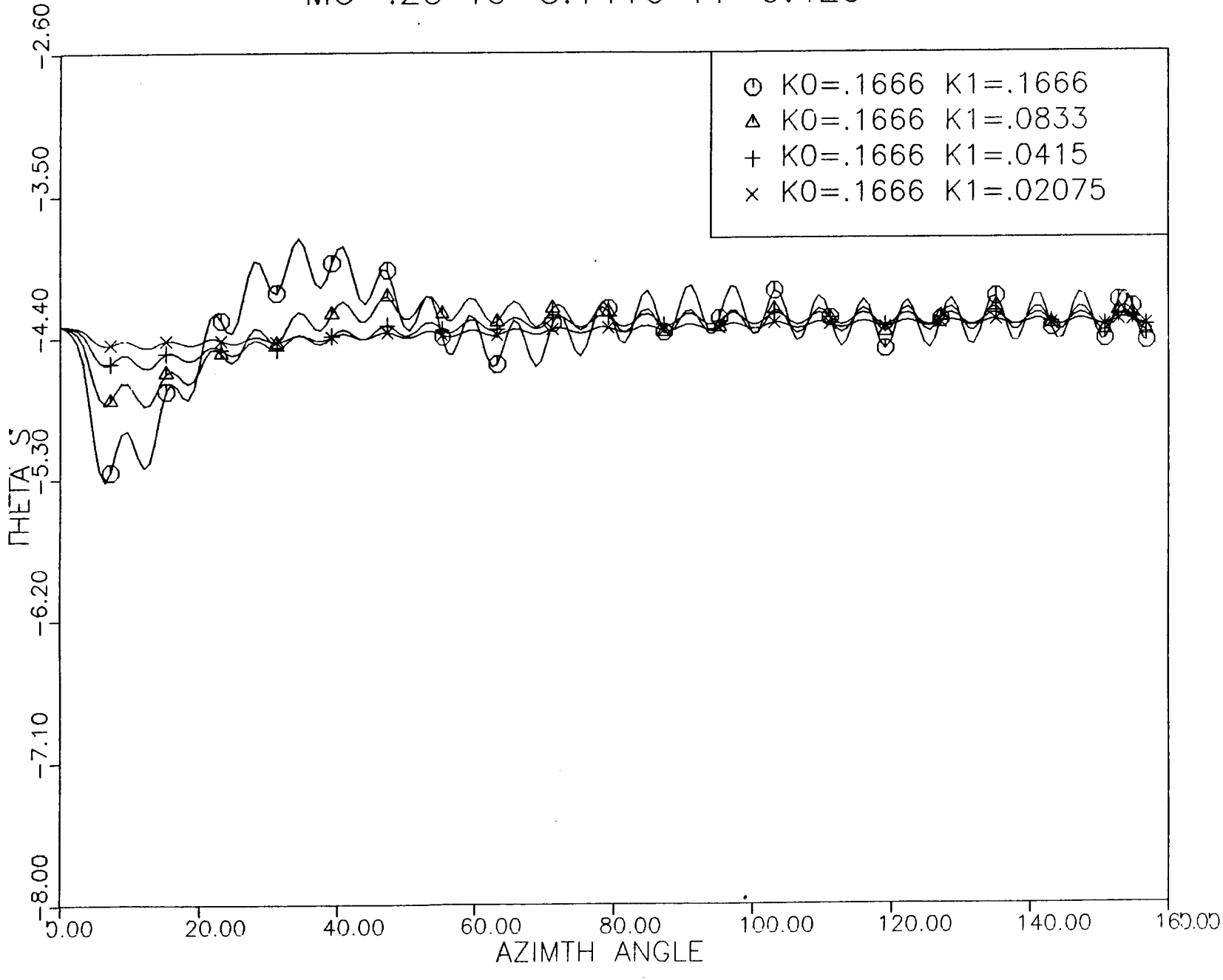

FIGURE 5c: AUTO–PILOT CONTROL

MU=.25 T0=3.1416 T1=9.425

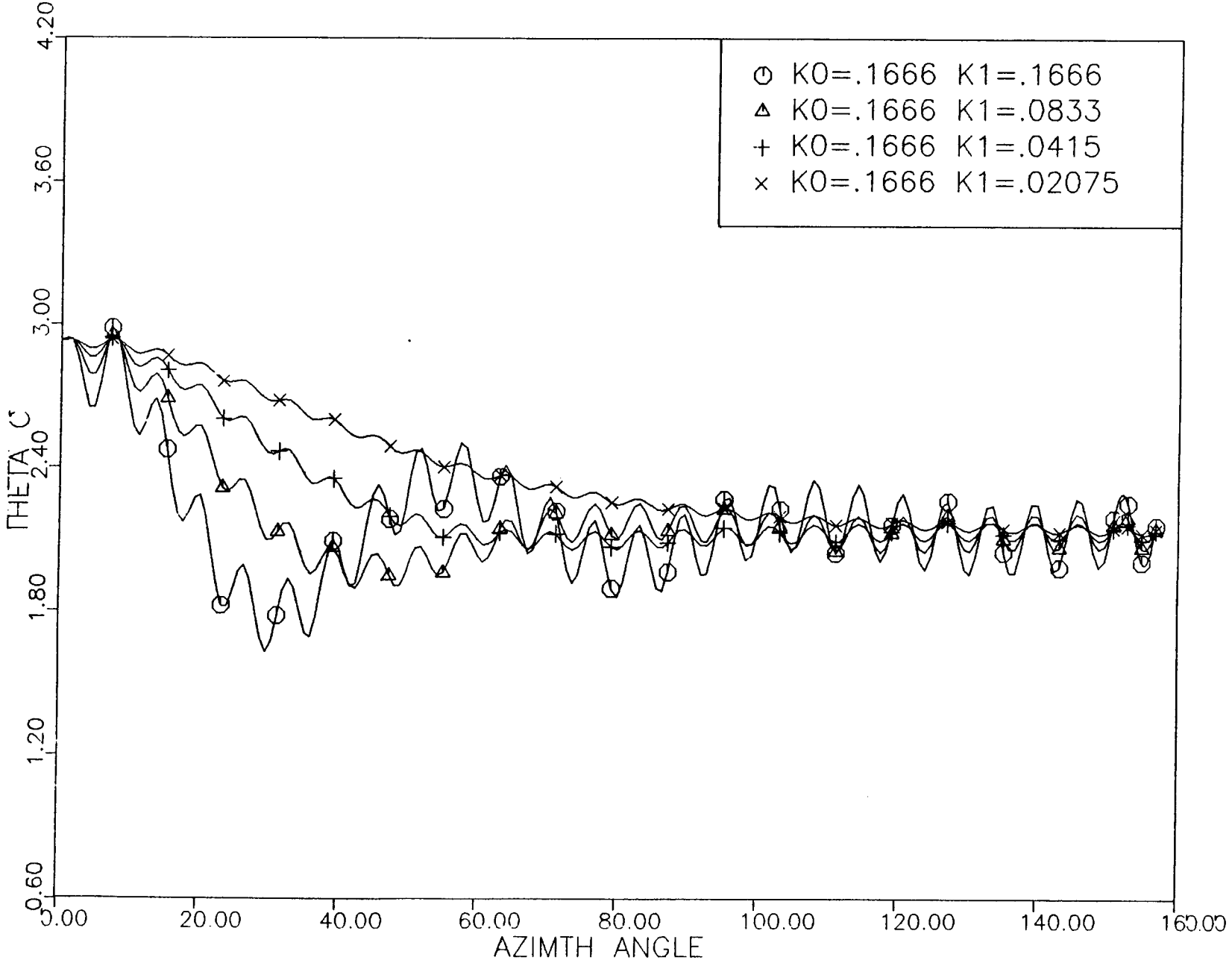

FIGURE 6a: AUTO-PILOT CONTROL

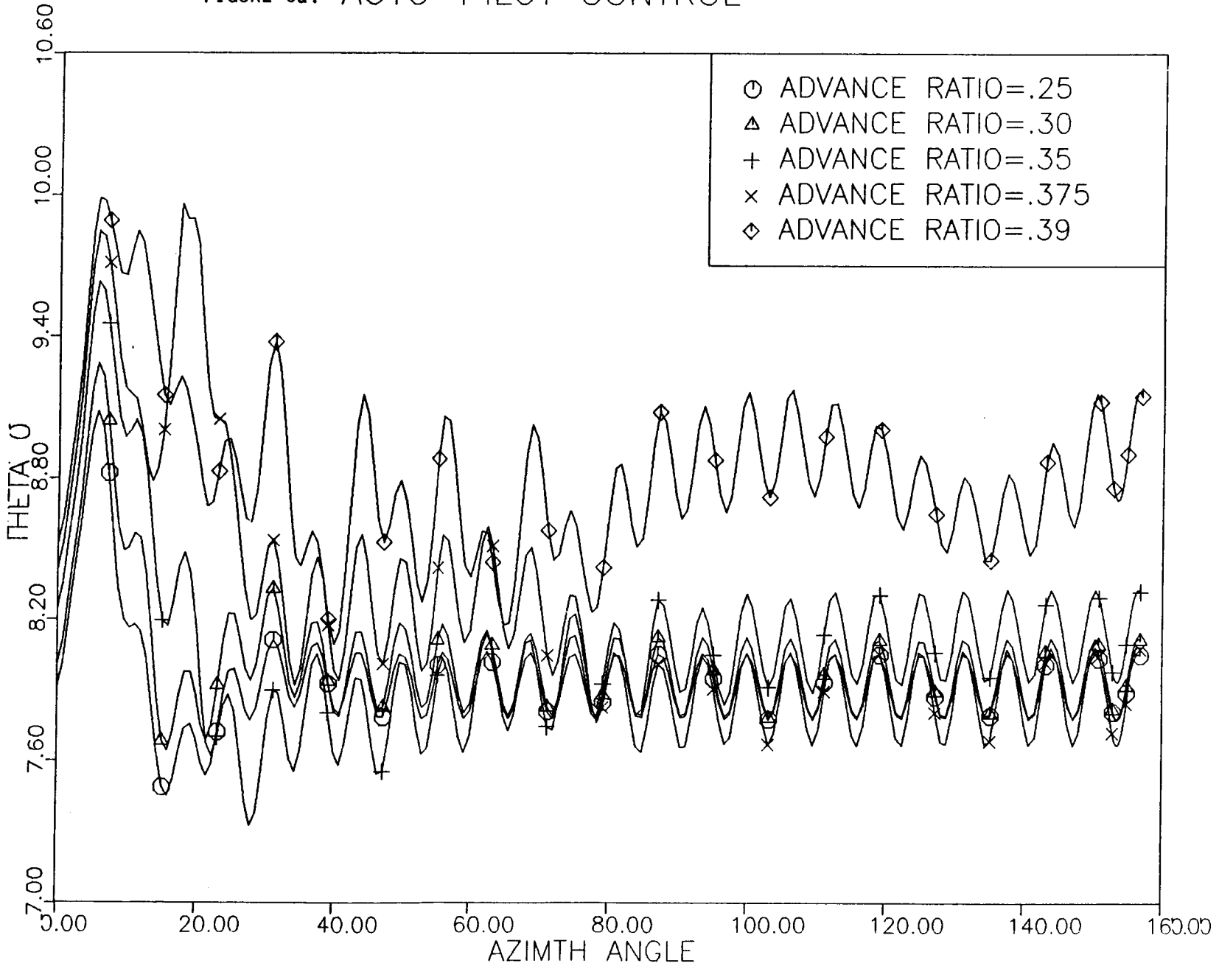

FIGURE 6b: AUTO–PILOT CONTROL

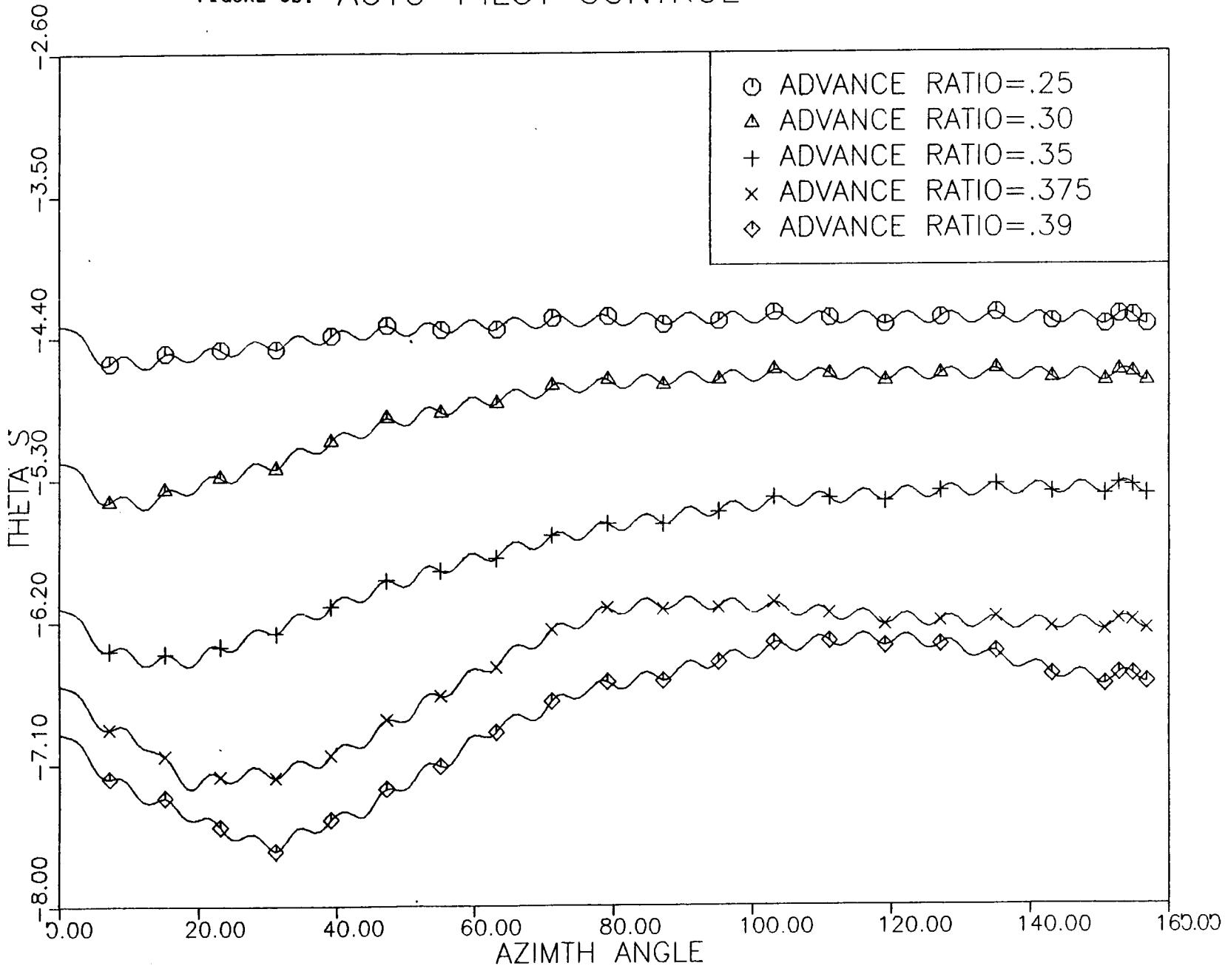

FIGURE 6c: AUTO–PILOT CONTROL

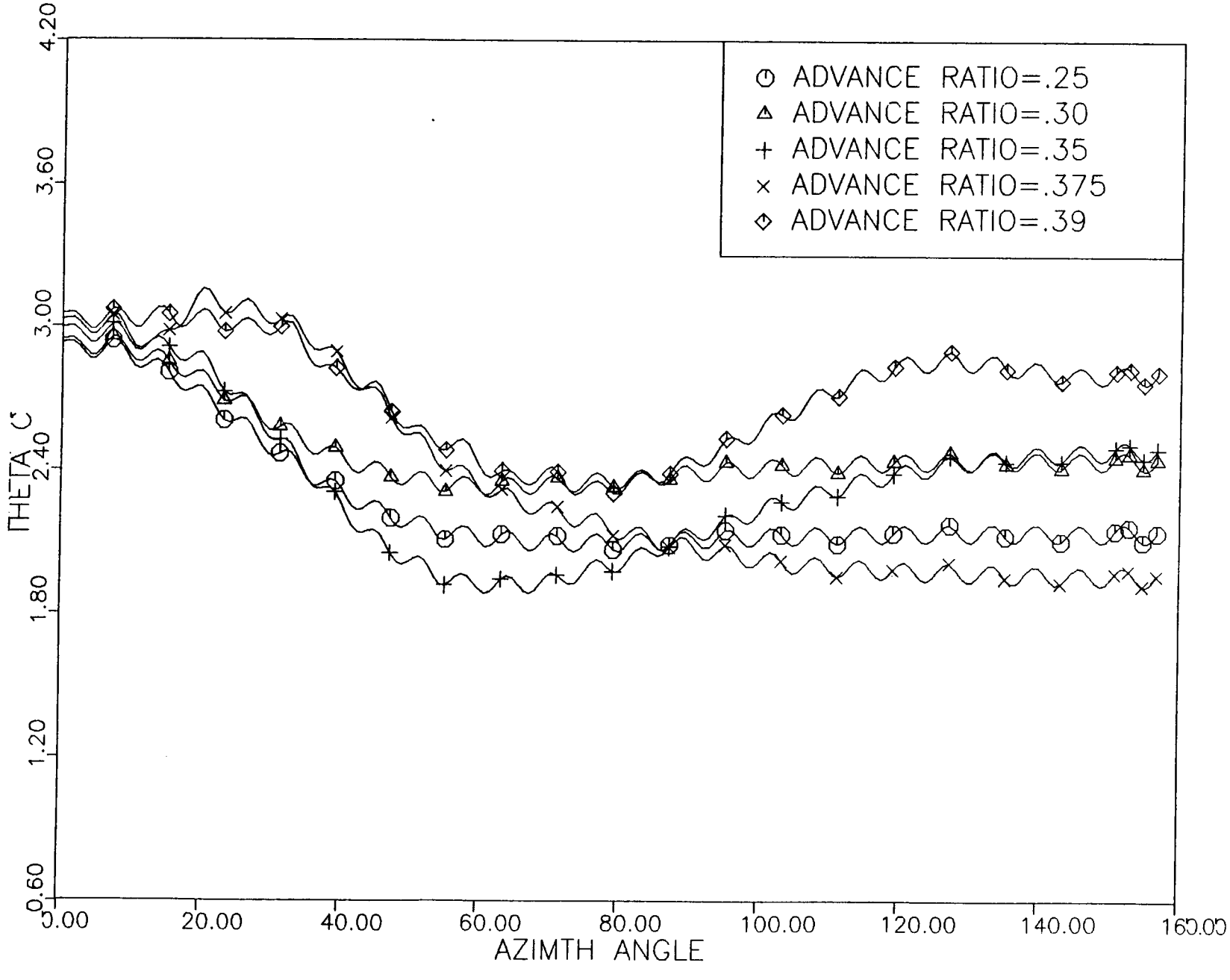

FIGURE 7a: FLAPPING RESPONSE

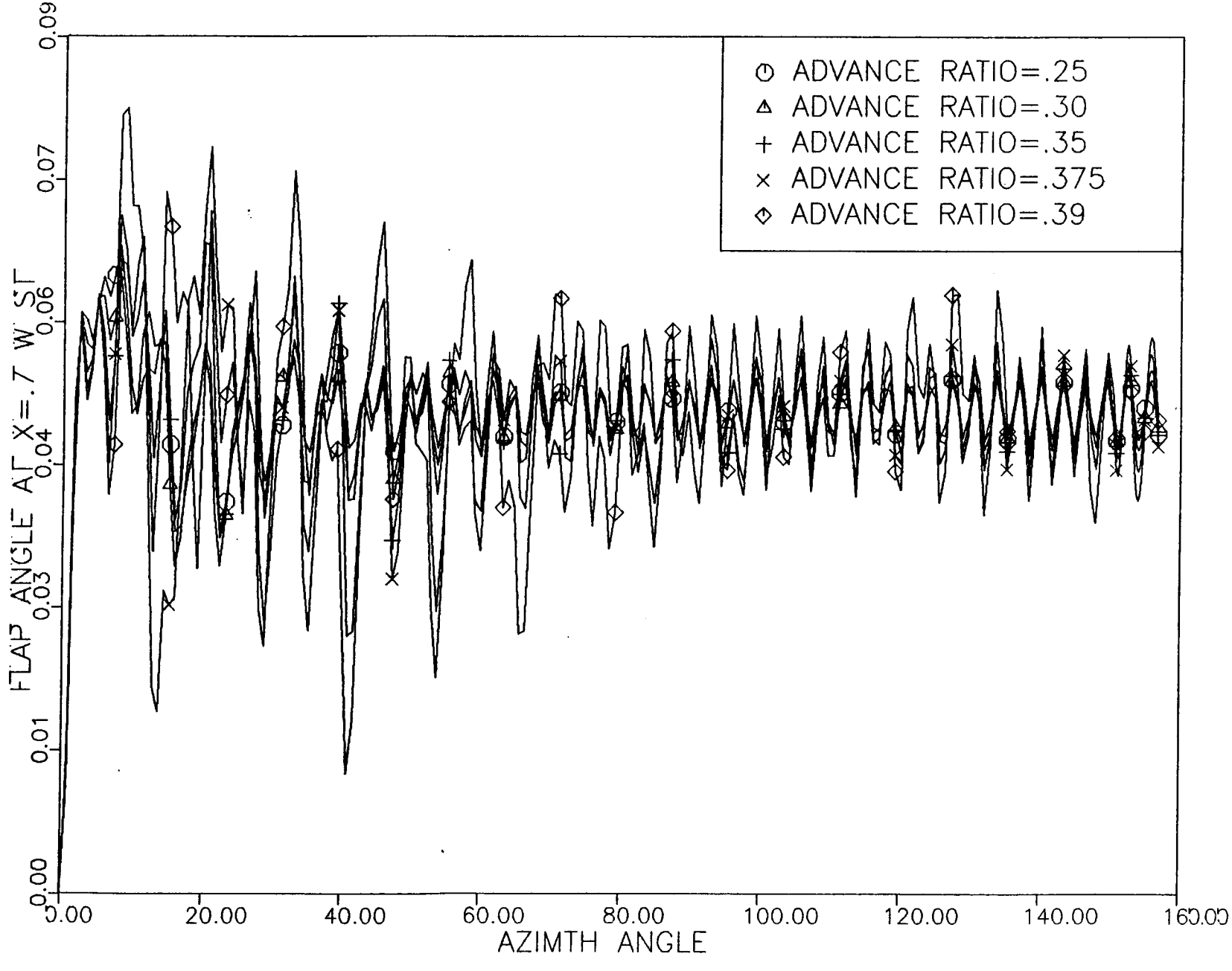

FIGURE 7b: FLAPPING RESPONSE